Characterization of Electrostriction Nonlinearity in a Standard Single-Mode Fiber Based on Coherent Detection and Cross-Phase Modulation

Rongqing Hui, *Senior Member, IEEE*, Charles Laperle, *Member, IEEE*, Michael Reimer, *Member, IEEE*, Andrew D. Shiner, *Member, IEEE*, and Maurice O'Sullivan

***Abstract*—The electrostriction nonlinearity in a standard single mode fiber is measured by cross-phase modulation (XPM) between pump and probe. Novel use of a coherent homodyne receiver allows measurement of in-phase and quadrature components of the probe field, eliminating the need for an optical interferometer. The Kerr effect (γ_k) and frequency-dependent electrostriction (γ_e) nonlinear parameters are characterized experimentally, and γ_e is found to be approximately one third of γ_k at the highest peak resonance frequency. The joint action of γ_k and γ_e also introduces a polarization dependence of the electrostrictive signal when the pump and the probe are not copolarized.**

***Index Terms*—Nonlinear optics, optical fiber communication, optical fiber measurements, optical fiber polarization.**

I. Introduction

OPTICAL fiber nonlinearity limits performance of fiber-optic communication systems [1]–[3]. In recent years, the availability of high speed digital signal processing has allowed equalization of fiber-related linear field propagation impairments, such as chromatic dispersion and polarization mode dispersion, in the electronic domain [4], [5]. However, the compensation of nonlinear effects has been less successful [6], [7]. Better understanding and more accurate characterization of fiber nonlinearities will help inform transceiver designs that must contend with their action. We present a measurement of the electrostrictive nonlinearity by means of coherent detection in an experiment with standard single mode fiber (SMF) that provides new insight into the polarization dependence of its effects.

Kerr effect nonlinearity is an intensity-dependent refractive index originating from the third-order susceptibility of the silica material. This femtosecond time scale process results in four-wave mixing within and between optical signals in a communication system. Electrostriction, on the other hand, is a process by which glass density depends on optical intensity. A time varying optical intensity excites sound waves in glass and the attendant index changes modulate the phase of the electric field. The frequency dependence of electrostriction in optical fiber is primarily determined by the mechanical properties of silica and the geometry of optical fiber [8], [9]. Acoustic standing waves can be created in the radial direction of the fiber in the frequency region <1 GHz by electrostriction. These acoustic waves propagate between the center and circumference of the cladding/coating interface [10]–[12], and modulate the refractive index of the fiber, resulting in phase modulation of a forward propagated optical signal.

The transverse acoustic wave created by the electrostriction, and its interaction with the optical signal, have been well studied [13], [14]. The consequent nonlinear coefficient can be evaluated by measuring the optical phase modulation of a probe wave created by the intensity modulation of a pump wave through cross-phase modulation (XPM). Normally, an optical interferometer is enlisted to convert probe phase modulation to intensity modulation for detection by a photodiode [15]–[18]. The accuracy of this system depends on the calibration of phase-to-intensity conversion efficiency of the interferometer as well as frequency response of the transmitter and the receiver transfer function. In this paper a coherent homodyne detection receiver capable of detecting both phase and amplitude of the optical field is used. The coherent detection receiver is also polarization selective, and thus the polarization-dependent complex nonlinear XPM crosstalk between pump and probe is characterized here without the need of an optical interferometer and the associated calibration. The polarization dependence of the electrostrictive signal is measured with this apparatus when the pump is polarized 45° from the probe. The polarization discrimination at the receiver also allows the elimination of the Kerr effect contribution to the XPM, while only selecting the contribution of electrostriction. This observed polarization dependence in the presence of electrostriction has not previously been reported in SMF, and is attributed to the frequency-dependent phase modulation which comprises real and imaginary parts of the electrostriction nonlinear parameter $\gamma_e(\Omega)$. An improved understanding of the admixture of Kerr and electrostriction nonlinearities is pertinent to the design and performance optimization of polarization multiplexed (PM) wavelength division multiplexed (WDM) coherent optical transmission systems. While direct detection systems are insensitive to optical phase noise at the receiver input, coherent systems use phase as a dimension for transmission and so are more vulnerable to such noise. Since electrostriction is limited

Manuscript received March 5, 2015; revised May 22, 2015; accepted July 6, 2015. Date of publication July 16, 2015; date of current version September 30, 2015. The work of R. Hui was supported in part by the US National Science Foundation under Grant 1409853.

R. Hui is with the Department of Electrical Engineering and Computer Science, University of Kansas, Lawrence, KS 66045 USA (e-mail: rhui@ku.edu).

C. Laperle, M. Reimer, A. D. Shiner, and M. O'Sullivan are with Ciena Corporation, Ottawa, ON K2H 8E9, Canada (e-mail: claperle@ciena.com; mreimer@ciena.com; ashiner@ciena.com; mosulliv@ciena.com).

Color versions of one or more of the figures in this paper are available online at http://ieeexplore.ieee.org.

Digital Object Identifier 10.1109/JLT.2015.2454475

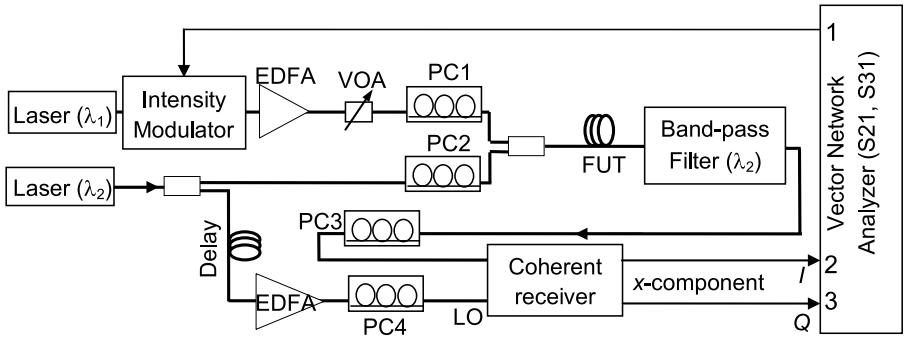

Fig. 1. Experimental setup for measuring the XPM crosstalk.

to low frequencies, $\Omega < 1$ GHz, systems with low symbol rates are more likely to register its effects. At 10 GBd, for example, $\gamma_e(\Omega)$ affects more than 10% of the channel spectrum. Even for higher symbol rates, its influence is present within and somewhat beyond the tracking bandwidth of a coherent receiver's carrier recovery. Finally, frequencies associated with overhead used to administer a channel, might otherwise unwittingly be chosen coincident with resonant frequencies of $\gamma_e(\Omega)$.

II. Experimental Setup and Theoretical Model

Both Kerr and electrostriction nonlinearities are evinced as intensity dependent refractive index, which can be measured by XPM in a pump-probe configuration as shown in Fig. 1. In this experimental setup, two single-polarization external-cavity tunable semiconductor lasers are used so that their wavelength separation can be adjusted. One of the lasers, emitting at 1550.26 nm, is a CW probe, the other, operating at 1550.63 nm, is an intensity modulated pump with modulation provided by a high speed $LiNbO_3$ electro-optic Mach-Zehnder modulator. The modulated pump power is amplified by an erbium-doped fiber amplifier (EDFA) before it is combined with the probe in a fiber coupler, and sent to the fiber under test (FUT). In this experiment, the FUT is a 25.257 km long standard SMF with a chromatic dispersion parameter $D = 17.5$ ps/nm/km, and an attenuation coefficient $\alpha = 0.23$ dB/km at the 1550 nm wavelength. An optical de-multiplexer ($\sim$0.32 nm bandwidth) at the output of the FUT rejects the pump before the coherent optical receiver. The local oscillator (LO) of the coherent optical receiver is tapped from the CW probe laser, undergoes a fiber delay line (having a comparable length to the FUT), and then is amplified by a second EDFA. The purpose of using the fiber delay line in the LO path is to reduce its relative delay to be within 10 m with respect to the probe that goes through the FUT, so that their relative phase variation is minimized for coherent homodyne detection. The coherent receiver includes a 90° optical hybrid and two photodiodes connected to transimpedance amplifiers with approximately 17 GHz bandwidth. A polarizer is used inside the coherent receiver to select a single polarization component from the probe optical signal. Four polarization controllers are used in the system: PC1 and PC2 adjust the state of polarization (SOP) of the pump and the probe at the FUT input, PC3 adjusts the SOP of the probe before it enters the coherent receiver, and PC4 ensures that the SOP of the local oscillator matches the polarizer orientation in the receiver. A RF vector network analyzer (RF-VNA) provides a frequency-swept signal that drives the electro-optic modulator to intensity modulate the pump and, simultaneously, captures the in-phase (I) and quadrature (Q) signals from the coherent receiver output.

Intensity modulation of the pump modulates the probe's optical phase via XPM in the FUT. At the same time, fiber chromatic dispersion converts some of the probe's phase modulation into intensity modulation. As the result, in principle both phase modulation and intensity modulation will be created on the probe wave at the FUT output. Following the principle of coherent homodyne detection with phase diversity [19], [20], the photocurrents at the I and Q outputs are:

$$dI(\Omega,t) = \eta_{pd}\left\{\delta A(\Omega)\cos\left[\varphi(t)\right] - A\delta\varphi(\Omega)\sin\left[\varphi(t)\right]\right\} \quad (1a)$$

$$dQ(\Omega,t) = \eta_{pd}\left\{\delta A(\Omega)\sin\left[\varphi(t)\right] + A\delta\varphi(\Omega)\cos\left[\varphi(t)\right]\right\} \quad (1b)$$

where, η_{pd} is the optoelectronic conversion efficiency which includes the photodiode responsivity, and the gain of the transimpedance amplifier. A and φ(t) are the average amplitude and slow varying phase of the probe, and $\delta A(\Omega)$ and $\delta\varphi(\Omega)$ are modulated components of amplitude and phase caused by the pump modulation at frequency Ω through XPM. The uncertainty of $\varphi(t)$ due to the phase noise of the probe is removed by squaring operations on the I and the Q components at the modulation frequency, so that the total RF power is independent of time,

$$\begin{aligned} P_{RF}(\Omega) &= dI^2(\Omega,t) + dQ^2(\Omega,t) \\ &= \eta_{pd}^2\left\{\delta A^2(\Omega) + \left[A\delta\varphi(\Omega)\right]^2\right\} \end{aligned} \quad (2)$$

Since $\delta A\cos\varphi \pm A\delta\varphi\sin\varphi = \sqrt{\delta A^2 + (A\delta\varphi)^2}\cos(\varphi \pm \delta)$, where $\delta = \tan^{-1}(\delta A/A\delta\varphi)$, and considering the random fluctuation of relative phase φ over time, a "maximum hold" operation on each input of the network analyzer provides the required P_{RF} at each frequency Ω, and simplifies the experiment and data processing. When the pump and the probe are co-polarized, the two terms on the right hand side of Eq. (2) contain the XPM-induced amplitude modulation and phase modulation, respectively, which can be calculated analytically as [21],

$$\delta A^2(\Omega) = 4\gamma^2 P_{LO} P_j P_k^2(\Omega)\left\{\frac{\exp(i\beta_2\Omega^2 L/2) - \exp(-\alpha + i\Omega d_{jk})L}{i(\alpha - i\Omega d_{jk} + i\beta_2\Omega^2 L/2)}\right.$$
$$\left. - \frac{\exp(-i\beta_2\Omega^2 L/2) - \exp(-\alpha + i\Omega d_{jk})L}{i(\alpha - i\Omega d_{jk} - i\beta_2\Omega^2 L/2)}\right\}^2 \quad (3)$$

and [22],

$$A^2\delta\phi^2(\Omega) = 16\gamma^2 P_{LO} P_j P_k^2(\Omega) \frac{\left(1-e^{-\alpha L}\right)^2}{\alpha^2+\Omega^2 d_{jk}^2} \left[1+\frac{4\sin^2\left(\Omega d_{jk} L/2\right) e^{-\alpha L}}{\left(1-e^{-\alpha L}\right)^2}\right] \quad (4)$$

where, L is the fiber length, $d_{jk} \equiv (1/v_j) - (1/v_k) \approx D \cdot (\lambda_j - \lambda_k)$ represents the pump/probe walk off, λ_j and λ_k are the wavelengths of the probe and the pump, v_j and v_k are the group velocities of the probe and the pump, $\beta_2 = -\lambda^2 D/(2\pi c)$ is the dispersion coefficient, α is the attenuation coefficient of the fiber, P_j and P_{LO} are the optical powers of the probe and the local oscillator at the receiver input, and $P_k(\Omega)$ is the pump power at the FUT input. The nonlinear parameter is $\gamma = 2\pi n_2/(\lambda A_{\text{eff}})$, where A_{eff} is the effective area of the fiber core, and $n_2 = n_{2k} + n_{2e}$ is the nonlinear refractive index, which includes a broadband Kerr effect contribution n_{2k} and a frequency-dependent electrostriction contribution $n_{2e}(\Omega)$. While n_{2k} is a material property which is independent of the fiber structure, $n_{2e}(\Omega)$ is jointly determined by the material property and the fiber structure. It is thus more convenient to separate the nonlinear parameter into $\gamma = \gamma_k + \gamma_e(\Omega)$, with $\gamma_k = 2\pi n_{2k}/(\lambda A_{\text{eff}})$, and $\gamma_e(\Omega) = 2\pi n_{2e}(\Omega)/(\lambda A_{\text{eff}})$, representing Kerr effect and electrostriction contributions, respectively.

The XPM power transfer function measured by the vector network analyzer is defined as the ratio between $P_{RF}(\Omega)$ and the pump modulation proportional to $P_k^2(\Omega)$. The absolute value of this transfer function depends on the modulation efficiency of the pump, the photodiode responsivity, power of the local oscillator, and the RF gain inside the coherent receiver. Therefore proper calibration is required to obtain an accurate value of the nonlinear parameter γ.

III. Measurement of $\gamma_E(\Omega)$

Fig. 2(a) shows the normalized XPM transfer functions calculated for $L = 25.257$ km of standard SMF. The contributions due to amplitude modulation, $\delta A^2(\Omega)$ (dash-dotted line), and phase modulation, $A^2\delta\varphi^2(\Omega)$ (dashed line), are shown separately for comparison. While optical phase modulation (PM) in this XPM process is a direct result of the power-dependent refractive index, the generation of amplitude modulation (AM) on the probe requires chromatic dispersion in the fiber which converts PM into AM. The efficiency of PM to AM conversion has a high-pass characteristic in the low frequency region [21]. Moreover, the fiber used in the experiment was relatively short such that accumulated chromatic dispersion was small. Thus the AM contribution shown in Fig. 2(a) is at least 30 dB lower than the PM contribution at frequencies below 2 GHz. Theoretical results shown in Fig. 2(a) did not include electrostriction nonlinearity $\gamma_e(\Omega)$, and thus the calculated total XPM transfer function does not show fine spectral features at low frequencies ($\Omega < 1$ GHz). A measurement with a finer resolution in the frequency region below 1.5 GHz reveals details of the resonance

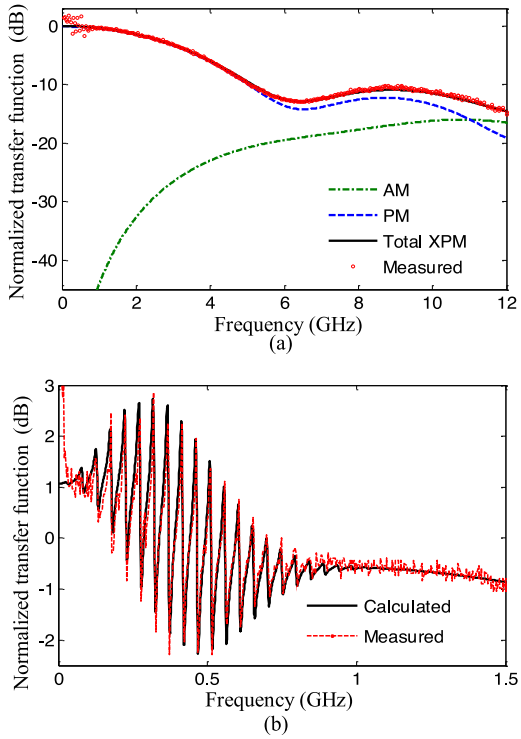

Fig. 2. (a): Normalized XPM transfer functions calculated with only AM contribution (dash-dotted line), only PM contribution (dashed line) and the combination of AM and PM contributions (solid line) without considering electrostriction nonlinearity. Red circles are measured XPM transfer function normalized to its lowest frequency value. (b): Calculated and measured XPM transfer function in the low frequency region when electrostriction nonlinearity is considered.

structure of the XPM transfer function due to electrostriction. This is shown in Fig. 2(b).

The calculation of electrostriction nonlinear parameter in the time domain is based on [11]:

$$\tilde{n}_{2e}(t) = U \sum_{m=1}^{\infty} B_m C_m e^{-\Gamma_m t} \frac{\sin(\Omega_m t)}{\Omega_m} \theta(t) \quad (5)$$

where,

$$B_m = -\frac{8\pi}{a^2} \int_0^R F_m(r) f(r) \left(1-\frac{r^2}{a^2}\right) r dr, \quad (6)$$

$$C_m = 2\pi \int_0^R F_m(r) f(r) r dr \quad (7)$$

and

$$\theta(t) = \begin{cases} 0 & t<0 \\ 1 & t>0 \end{cases}$$

$F_m(r) = M_m J_0(\mu_m r/R)$ is the radial acoustic wave eigenfunction, in which the eigenvalue μ_m can be obtained by solving:

$$\left[1-(v_s/v)^2\right] J_0(\mu_m) - (v_s/v_d)^2 J_2(\mu_m) = 0 \quad (8)$$

and the normalization factor M_m can be found with,

$$M_m = \frac{1}{R\sqrt{\pi[J_0^2(\mu_m) + J_1^2(\mu_m)]}} \tag{9}$$

where, v_d and v_s are longitudinal and shear sound velocities. J_0, J_1, and J_2 are the 0th, 1st and 2nd order Bessel functions, respectively. a is the effective core radius, and R is the cladding radius of the fiber. The frequency of the mth acoustic mode is $\Omega_m = \mu_m v_d/R$, and Γ_m is the damping rate. $f(r) = \exp\left(-r^2/2a^2\right)$ is the transversal distribution of the optical field in the fiber. Finally, $\tilde{n}_{2e}(t)$ can be converted into frequency domain through a simple Fourier transform to obtain $n_{2e}(\Omega)$. Note that in Eq. (5), the proportionality coefficient U is determined by a number of material properties of the fiber core, cladding and the nature of cladding/coating interface [10], [11].

We used the following SMF parameter values for the calculation: $v_s = 3740$ m/s, $\Gamma_m = 3 \times 10^7$ s^{-1}, $a = 3.6$ μm, and $R = 62.5$ μm. The shear sound velocity $v_d = 5970$ m/s was used to obtain the best fit with the measured electrostriction resonance frequencies, which is slightly higher than the value (5910 m/s) used in [12]. The Kerr effect nonlinearity in standard SMF is approximately $n_{2k} = 2.2 \times 10^{-20}$ m^2/W [23], corresponding to $\gamma_k = 1.1$ W^{-1}km^{-1} for SMF. Here we find the value of $\gamma_e(\Omega)$ relative to γ_k.

At high frequencies ($\Omega > 1$ GHz in Fig. 2) the XPM transfer function only depends on the Kerr effect nonlinearity γ_k. Below 1 GHz in Fig. 2, it depends on a combination of Kerr effect and electrostriction nonlinearities. Using $\gamma = \gamma_k + \gamma_e(\Omega)$ in Eqs. (3) and (4), the XPM transfer function can be calculated. The proportionality coefficient U in Eq. (5) can be adjusted once to obtain the best fit between the calculated and the measured XPM transfer functions for both high ($\Omega >1$ GHz) and low ($\Omega <1$ GHz) frequency regions as shown in Fig. 2. Although this optimum fitting only guarantees the correct ratio of $\gamma_e(\Omega)/\gamma_k$, it avoids complications due to a number of calibration uncertainties such as pump power levels, modulator response, and receiver electro-optic conversion efficiency. Fig. 3 shows the real and the imaginary parts of $\gamma_e(\Omega)$ calculated from Eq. (5) with $U = 5 \times 10^{-15}$, which resulted in the best fit to the measured XPM transfer function as shown in Fig. 2(b), where $\gamma_k = 1.1$ W^{-1}km^{-1} was assumed, corresponding to the experimental condition of co-polarized pump and probe. Note that this γ_k value is dependent on the fiber type.

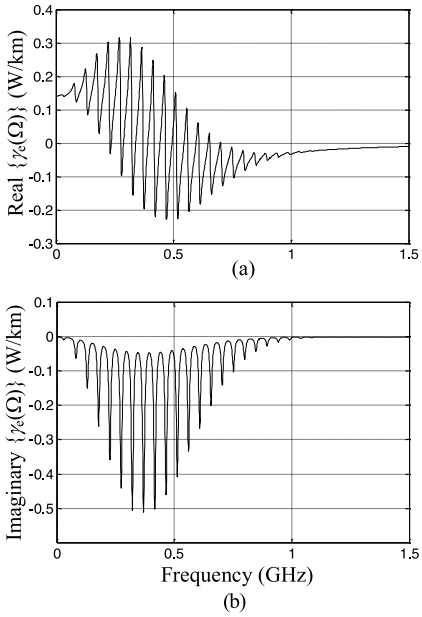

Fig. 3. Calculated real (a) and imaginary (b) parts of $\gamma_e(\Omega)$ through best fitting to the measured XPM transfer function. $U = 5 \times 10^{-15}$.

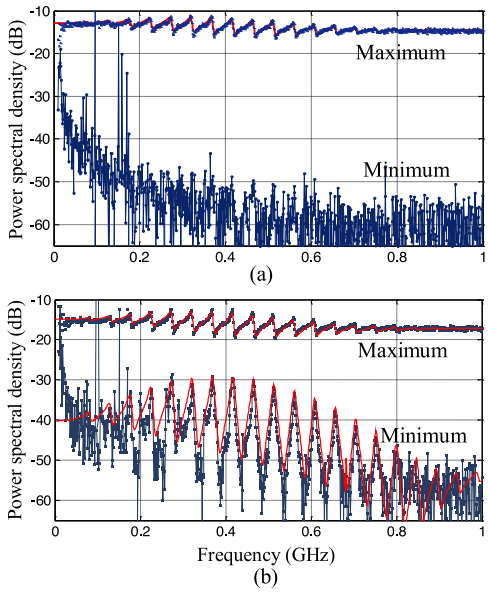

Fig. 4. Measured maximum and minimum transfer functions of XPM crosstalk (blue dots) with 9.57 dBm pump average power at FUT input. (a) pump was co-polarized with the probe, and (b) there was 45° polarization mismatch between pump and probe at fiber input. Red continuous lines were calculated.

IV. Residual Intensity Modulation and Impact on Cross-Polarization Modulation

Because of the axial symmetry of the optical field in the fiber and the symmetry of acoustic standing waves in the transversal direction, it is generally accepted that electrostriction nonlinearity does not contribute to the polarization state change of the probe optical signal. However, we observe a polarization dependence of our signal that is caused by electrostriction. In the experimental setup shown in Fig. 1, the coherent receiver is polarization-selective, in which both the LO and the probe optical signals are selected by a polarizer. By adjusting the polarization controller PC4, the SOP of the LO matches the orientation of the receiver polarizer so that the LO power at the photodiode is always maximized. The SOP of the probe can be independently adjusted by PC3 before it reaches the polarization analyzer in the coherent receiver.

Fig. 4 shows the spectra of XPM crosstalk measured with 9.57 dBm average pump power at the fiber input. Fig. 4(a) was obtained with co-polarized pump and probe set by PC1 and PC2 at the FUT input. By adjusting PC3 at the receiver input, the SOP of the probe can be made parallel or perpendicular with respect to the axis of the receiver polarizer, and thus the

spectral density of XPM crosstalk measured by the network analyzer could be maximized or minimized, shown as blue dots in Fig. 4(a) marked with maximum and minimum, respectively. The red solid line in Fig. 4(a) was calculated based on Eqs. (2)–(4) using $\gamma_k = 1.1\ \mathrm{W^{-1}km^{-1}}$ and $\gamma_e(\Omega)$ values shown in Fig. 3. The electro-optic conversion efficiency of the receiver was adjusted so that the level of the calculated spectral density best fits to the measured maximum transfer function at 1 GHz. In this configuration, proper adjustment of PC3 allowed cancellation of XPM crosstalk on the probe at the pump modulation frequency caused by Kerr effect and electrostriction nonlinearities combined. Except for 1/f noise at low frequency ($\Omega <$ 0.2 GHz), the trace of the minimum measured spectral density shown in Fig. 4(a) is at the instrument's noise floor. This clearly shows that the probe wave was not depolarized by either Kerr or electrostriction nonlinear processes when pump and probe polarizations are aligned.

In a second measurement, the SOP of the pump was rotated by 45° with respect to the probe at the FUT input, and thus the XPM efficiency due to the Kerr effect nonlinearity was reduced by a factor of 2/3 compared to that with co-polarized pump and probe. Thus, the power spectral density shown as "maximum" trace in Fig. 4(b) is approximately 3.5dB lower than that in Fig. 4(a) at 1 GHz where Kerr effect nonlinearity dominates. Meanwhile, since the XPM crosstalk due to electrostriction nonlinearity is independent of pump/probe SOP mismatch in the fiber, the relative contribution of electrostriction increases. This is shown as the increased peak-to-peak excursion (in dB) of the resonance structure in the "maximum" XPM transfer function of Fig. 4(b) compared to that in Fig. 4(a). In contrast with the co-polarized experiment, we observe in Fig. 4(b) that when the XPM crosstalk due to Kerr effect nonlinearity is eliminated by adjusting PC3 to minimize the XPM crosstalk for frequencies >1 GHz at the receiver, a residual resonance structure in the XPM transfer function is still apparent below 1GHz. This is shown in the lower trace marked with "minimum". Thus, the receiver polarizer did not remove all of the probe power at the receiver in this particular situation, and residual electrostriction signal at the modulation frequency was detected, even though Kerr effect contribution to XPM was completely removed. This suggests that the SOP of the probe might be modified by the frequency-dependent electrostriction nonlinearity.

Stress birefringence has been found in a vibrating cylinder, and birefringence patterns have been presented and analyzed [13]. This also applies to guided acoustic modes produced by electrostriction nonlinearity in an optical fiber. Polarization rotation of the probe wave due to electrostriction can only be introduced by the mixed modes of the acoustic wave which causes stress dependent on the azimuthal angle [14]. However, in our measurement based on a standard SMF with a high degree of axial symmetry, only resonance structures corresponding to radial modes were observable in the measured XPM transfer function shown in Figs. 2 and 4, which agrees well with that predicted by Eq. (5) where only radial modes are considered. Although Kerr effect nonlinearity can introduce cross-polarization modulation in the probe when it has a 45° polarization angle with respect to the pump, the probe power can still be eliminated by a polarizer at the receiver. However, the frequency dependent electrostrictive phase common to both polarizations modifies the optimum extinction angle of the receiver polarizer which results in an observed leak of the probe field as shown in the "minimum" trace of Fig. 4(b). The strong resonance structure of the spectrum in the "minimum" trace of Fig. 4(b) is attributed to the phase modulation caused by electrostriction.

To explain this observation, we consider a horizontally linear polarized pump, and assume the probe is also linear polarized but at a 45° angle with respective to the pump. The field vector of the probe is $\vec{E} = A\left[1\ 1\right]^T/\sqrt{2}$, where A is the field amplitude and T denotes matrix transpose. Assuming the principal axis of the receiver polarizer is set along the horizontal direction x, the probe field that reaches the receiver can be expressed as,

$$\begin{bmatrix} E_x(t) \\ E_y(t) \end{bmatrix} = \begin{bmatrix} 1 & 0 \\ 0 & 0 \end{bmatrix} \begin{bmatrix} \cos\theta & e^{i\phi}\sin\theta \\ -e^{-i\phi}\sin\theta & \cos\theta \end{bmatrix} \times \begin{bmatrix} e^{i\gamma_x p_k(t)} & 0 \\ 0 & e^{-i\gamma_x p_k(t)} \end{bmatrix} e^{i[\gamma_c P_k(t) + \tilde{\gamma}_e(t) \otimes p_k(t)]} \begin{bmatrix} 1 \\ 1 \end{bmatrix} \frac{A}{\sqrt{2}} \tag{10}$$

On the right hand side of Eq. (10), the first term represents the receiver polarizer, the second term is the Jones matrix of the polarization controller (PC3), and the third term represents birefringence caused by the Kerr effect cross-polarization modulation with $\gamma_x = \pi n_{2k} L_{\mathrm{eff}} / (\lambda A_{\mathrm{eff}})$ [24]. $e^{i[\gamma_c p_k(t) + \tilde{\gamma}_e(t) \otimes p_k(t)]}$ is a nonlinear phase modulation which depends on both the Kerr effect nonlinear parameter $\gamma_c = 3\pi n_{2k} L_{\mathrm{eff}} / (\lambda A_{\mathrm{eff}})$ and the time-dependent electrostriction nonlinearity $\gamma_e(\Omega)$. The symbol "$\otimes$" represents a convolution, and $p_k(t)$ is the pump modulation waveform.

When the pump power is modulated by a sinusoid, $p_k(t) = p_{k0}(1 + \cos\Omega t)$, the fundamental tone imparted to the probe by Kerr effect XPM can be eliminated by a polarizer at the receiver provided proper polarization pre-conditioning. To minimize the fundamental tone on the probe field, the parameters of the polarization controller in Eq. (10) can be obtained using the Jacobi-Anger identity:

$$\theta = -\tan^{-1}\left\{\frac{J_1[p_{k0}(\gamma_c + \gamma_x)]}{J_1[p_{k0}(\gamma_c - \gamma_x)]}\right\} \tag{11a}$$

$$\phi = 2\gamma_x p_{k0} \tag{11b}$$

While the efficiency of electrostriction $\gamma_e(\Omega)$ is independent of the SOP, it is strongly frequency-dependent in the low frequency region ($\Omega <$ 1GHz). The convolution in the common phase term in Eq. (10) can be expressed as $\tilde{\gamma}_e(t) \otimes p_k(t) = p_{k0}\left[\gamma_e^r(0) + \gamma_e^r(\Omega)\cos\Omega t - \gamma_e^i(\Omega)\sin\Omega t\right]$, where $\gamma_e^r(\Omega)$ and $\gamma_e^i(\Omega)$, are the real and the imaginary parts of $\gamma_e(\Omega)$, respectively. The presence of electrostriction makes the optimum polarization angle θ described in Eq. (11) frequency dependent, and thus the probe field cannot be completely eliminated by a polarizer. The leaked-through $E_x(t)$ component in Eq. (10), phase modulated at the frequency Ω, is detected by the coherent receiver and RF-VNA. The continuous line in Fig. 4(b) "minimum" shows the Fourier transform of $E_x(t)$ obtained with

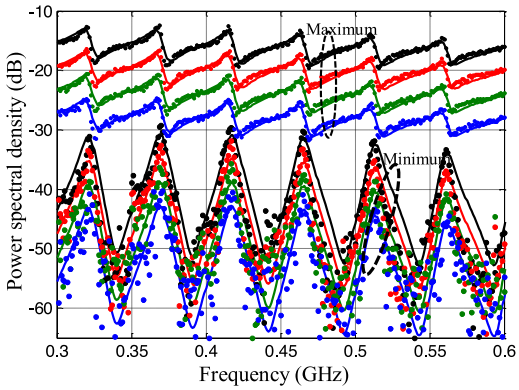

Fig. 5. Measured (symbols) and calculated (solid lines) maximum and minimum transfer functions of XPM crosstalk with pump power level of 9.57 dBm (black), 7.58 dBm (red), 5.58 dBm (green) and 3.5 dBm (blue) at the fiber input. Maximum and minimum traces were obtained by maximizing or minimizing Kerr effect nonlinearity contribution by means of polarization controller P C3.

Eqs. (10) and (11) and by scanning the modulating frequency Ω. The calculated results agree reasonably well with the measured spectrum.

Note that when the pump and probe are co-polarized, this residual signal modulation is blocked by the receiver polarizer which minimizes the probe optical field. For example, if the pump and the probe are both linear horizontal polarized, the probe is $\vec{E} = A\begin{bmatrix}1 & 0\end{bmatrix}^T$, and $E_x(t)$ in Eq.(10) is proportional to $\cos(\theta)$ which can be completely eliminated with a polarizer by setting $\theta = \pi/2$. This explains why the resonance structure of the XPM transfer function does not exist in the "minimum" trace of Fig. 4(a).

Under the same conditions used to obtain Fig. 4(b), we further measured the "maximum" and "minimum" XPM transfer functions at different average power levels of the pump. Fig. 5 indicates that for every 2 dB decrease of average pump power, both the "maximum" and the "minimum" XPM transfer functions are reduced by 4 dB. The ratio (or the difference in dB) between the corresponding "maximum" and "minimum" traces is relatively independent of the pump power level. This observation is also reproducible by the calculation based on Eqs. (10) and (11).

V. Conclusion

We have measured the contributions of Kerr effect and electrostriction nonlinearities in a SMF by means of XPM in a pump-probe configuration. A coherent homodyne receiver was used which allowed the simultaneous detection of both the amplitude and the phase of the optical signal in the probe channel. The measured and calculated XPM transfer functions are in good agreement. The frequency-dependent electrostriction nonlinear parameter introduces resonance structure of cross-phase modulation originating from the radial modes of the acoustic wave in the fiber. We have observed that when pump and probe channels are not co-polarized, the frequency dependent electrostriction modifies the angle of extinction of the receiver polarizer. When this is the case XPM crosstalk due to Kerr effect and electrostriction cannot be simultaneously removed by a polarizer at the receiver input. We have reproduced these observations with a simple model of our experiment.

References

[1] G. P. Agrawal, *Nonlinear Fiber Optics*. New York, NY, USA: Academic, 2007.
[2] A. R. Chraplyvy, "Limitations on lightwave communications imposed by optical-fiber nonlinearities," *J. Lightw. Technol.*, vol. 8, no. 10, pp. 1548–1557, Oct. 1990.
[3] R. H. Stolen, "Nonlinearity in fiber transmission," *Proc. IEEE*, vol. 68, no. 10, pp. 1232–1236, Oct. 1980.
[4] J. McNicol, M. O'Sullivan, K. Roberts, A. Comeau, D. McGhan, and L. Strawczynski, "Electrical domain compensation of optical dispersion," presented at the Optical Fiber Communication Conf., Anaheim, CA, USA, 2005, Paper OThJ3.
[5] K. Roberts, M. O'Sullivan, K.-T. Wu, H. Sun, A. Awadalla, D. Krause, and C. Laperle, "Performance of dual-polarization QPSK for optical transport systems," *J. Lightw. Technol.*, vol. 27, no. 16, pp. 3546–3559, Aug. 2009.
[6] X. Liu, F. Buchali, and R. W. Tkach, "Improving the nonlinear tolerance of polarization-division-multiplexed CO-OFDM in long-haul fiber transmission," *J. Lightw. Technol.*, vol. 27, no. 16, pp. 3632–3640, Aug. 2009.
[7] K. Roberts, C. Li, L. Strawczynski, M. O'Sullivan, and I. Hardcastle, "Electronic pre-compensation of optical nonlinearity," *IEEE Photon. Technol. Lett.*, vol. 18, no. 2, pp. 403–405, Jan. 2006.
[8] E. P. Ippen and R.H. Stolen, "Stimulated Brillouin scattering in optical fibers," *Appl. Phys. Lett.*, vol. 21, no. 539, pp. 539–541, 1972.
[9] Y. Aoki, K. Tajima, and I. Mito, "Input power limits of single-mode optical fibers due to stimulated Brillouin scattering in optical communication systems," *J. Lightw. Technol.*, vol. 6, no. 5, pp. 710–719, May 1988.
[10] E. M. Dianov, A. V. Luchnikov, A. N. Pilipetskii, and A. N. Starodumov, "Long-range interaction of soliton pulse trains in a single mode fiber," *Soviet Lightw. Commun.*, vol. 1, no. 1, pp. 37–43, 1991.
[11] E. M. Dianov, A. V. Luchnikov, A. N. Pilipetskii, and A. M. Prokhorov, "Long-range interaction of picosecond solitons through excitation of acoustic waves in optical fibers," *Appl. Phys. B*, vol. 54, pp. 175–180, 1992.
[12] A. Melloni, M. Martinelli, and A. Fellegara, "Frequency characterization of the nonlinear refractive index in optical fiber," *Fiber Integr. Opt.*, vol. 18, no. 1, pp. 1–13, 1999.
[13] E. K. Sittig and G. A. Coquin, "Visualization of plane-strain vibration modes of a long cylinder capable of producing sound radiation," *J. Acoustical Soc. Amer.*, vol. 48, no. 5, pp. 1150–1159, 1970.
[14] R. M. Shelby, M. D. Levenson, and P. W. Bayer, "Guided acoustic-wave Brillouin scattering," *Phys. Rev. B*, vol. 31, no. 8, pp. 5244–52, 1985.
[15] E. L. Buckland and R. W. Boyd, "Electrostrictive contribution to the intensity-dependent refractive index of optical fibers," *Opt. Lett.*, vol. 21, no. 15, pp. 1117–1119, 1996.
[16] E. L. Buckland and R. W. Boyd, "Measurement of the frequency response of the electrostrictive nonlinearity in optical fibers," *Opt. Lett.*, vol. 22, no. 10, pp. 676–678, 1997.
[17] A. Melloni, M. Frasca, A. Garavaglia, A. Tonini, and M. Martinelli, "Direct measurement of electrostriction in optical fibers," *Opt. Lett.*, vol. 23, no. 9, pp. 691–693, 1998.
[18] A. Fellegara, A. Melloni, and M. Martinelli, "Measurement of the frequency response induced by electrostriction in optical fibers," *Opt. Lett.*, vol. 22, no. 21, pp. 1615–1617, 1998.
[19] R. Hui and M. O'Sullivan, *Fiber-Optic Measurement Techniques*. Boston, MA, USA: Academic, 2009.
[20] K. Kikuchi, "Phase-diversity homodyne detection of multilevel optical modulation with digital carrier phase estimation," *IEEE J. Sel. Top. Quant. Electron.*, vol. 12, no. 4, pp. 563–570, Jul./Aug. 2006.
[21] R. Hui, K. Demarest and C. Allen, "Cross phase modulation in multispan WDM optical fiber systems," *J. Lightw. Technol.*, vol. 17, no. 7, pp. 1018–1026, Jun. 1999.
[22] T.-K. Chiang, N. Kagi, M. E. Marhic, and L. Kazovsky, "Cross-phase modulation in fiber links with multiple optical amplifiers and dispersion compensators," *J. Lightw. Technol.*, vol. 14, no. 3, pp. 249–260, Mar. 1996.
[23] A. Boskovic, S. V. Chernikov, J. R. Taylor, L. Gruner-Nielsen, and O. A. Levring, "Direct continuous-wave measurement of n_2 in various types of telecommunication fiber at 1.55 μm," *Opt. Lett.*, vol. 21, pp. 1966–1968, 1996.
[24] M. Winter, C.-A. Bunge, D. Setti, and K. Petermann, "A statistical treatment of cross-polarization modulation in DWDM systems," *J. Lightw. Technol.*, vol. 27, no. 17, pp. 37398–3751, Sep. 2009.

Rongqing Hui (M'94–SM'97) received the B.S. and M.S. degrees from the Beijing Institute of Posts and Telecommunications, Beijing, China, and the Ph.D. degree from Politecnico di Torino, Turin, Italy, all in electrical engineering. He is a Professor of electrical engineering and computer science at the University of Kansas, Lawrence, KS, USA. Before joining the faculty of the University of Kansas in 1997, he was a Member of the Scientific Staff, Bell-Northern Research, and then Nortel, where he worked in research and development of high-speed optical transport networks. He served as a Program Director at the US National Science Foundation for two years from 2006 to 2007, where he was in charge of research programs in photonics and optoelectronics. He has published more than 100 journal papers in addition to numerous conference papers in the area of fiber-optic systems and devices, and holds 16 US patents. He served as a Topic Editor for the IEEE TRANSACTIONS ON COMMUNICATIONS from 2001 to 2007, and an Associate Editor for the IEEE JOURNAL OF QUANTUM ELECTRONICS from 2006 to 2013.

Charles Laperle (M'90) received the B.Eng. degree from Sherbrooke University, Sherbrooke, QC, Canada, in 1991, the M.Eng. degree from McMaster University, Hamilton, ON, Canada, in 1993, and the Ph.D. degree from Laval University, Québec, QC, in 2003, all in electrical engineering. He was with the Wireless Development Group, Nortel, Canada, from 1997 to 2000, as an RF Hardware Designer for TDMA wireless base stations. He was with the Optical Research and Development Group, Nortel, as an electro-optic hardware designer from 2001 to 2010. He has been with Ciena Corporation, Ottawa, ON, since 2010 as an Optical Systems Designer. His current activities include the development of DSP-assisted coherent transceivers for next-generation optical communication systems for 100 Gb/s and beyond. He was a Technical Committee Member of OFC/NFOEC from 2010 to 2012.

Michael Reimer, biography not available at the time of publication.

Andrew D. Shiner (M'06) received the B.Eng. degree in engineering physics from McMaster University, Hamilton, ON, Canada, in 2004. He received the M.Sc. degree from York University, Toronto, ON, in 2006. He received the Ph.D. degree from the Joint University of Ottawa/NRC Attosecond Laboratory (JASLAB), Ottawa, ON, in 2013, in the area of extreme nonlinear optics. He joined Ciena Corporation, Ottawa, as a Systems Engineer in 2012, with research activities that include the study of nonlinear propagation in telecommunications fibers, advanced constellation design and carrier recovery.

Maurice O'Sullivan, biography not available at the time of publication.